Scientific Research Journal,
Vol 20, No 2 (2023) 53-69
https://doi.org/10.24191/srj.v20i2.22185

Revival of Ferromagnetic-Metallic Phase and Emergence of Griffiths Phase via Ni and Cr Substitution in Charged-Ordered $Pr_{0.75}Na_{0.25}MnO_3$ Manganite

Rozilah Rajmi[1*], Norazila Ibrahim[2], Zakiah Mohamed[2]
Siti Sumaiyah Sheikh Abdul Aziz[3]

[1]Faculty of Applied Sciences, Universiti Teknologi MARA (UiTM) Cawangan Perlis, Campus Arau, 02600 Arau, Perlis, Malaysia
[2]Faculty of Applied Sciences, Universiti Teknologi MARA (UiTM), 40450 Shah Alam, Selangor, Malaysia.
[3]Faculty of Applied Sciences, Universiti Teknologi MARA (UiTM), Perak Branch, Tapah Campus, 35400 Tapah Road, Perak, Malaysia

**Corresponding Author's E-mail: rozilahrajmi@uitm.edu.my*

Received: 17 April 2023
Accepted: 19 June 2023
Online First: 21 September 2023

ABSTRACT

Polycrystalline samples of $Pr_{0.75}Na_{0.25}Mn_{1-x}A_xO_3$ (A = Ni, Cr; x = 0, 0.03) were prepared using conventional solid-state method and their structural and magnetic properties were investigated. Monovalent-doped $Pr_{0.75}Na_{0.25}MnO_3$ exhibits insulating behavior which is related to the strong localization of charge carriers due to the presence of charge ordering (CO). The substitution of different of magnetic ions, A, which are Ni^{2+} and Cr^{3+}, at a concentration of x = 0.03 at the Mn site in the CO $Pr_{0.75}Na_{0.25}Mn_{1-x}A_xO_3$ manganite, has been found to dramatically modify its structural and magnetic properties. X-ray diffraction patterns showed that all samples were present in single phase and crystallized in orthorhombic structure with Pnma space group. The Rietveld refinement analysis showed that the unit cell volume increased due to Ni^{2+} substitution, while it decreased due to Cr^{3+} substitution, which may be attributed to the different ionic radii of both ions. The suppression of the CO state and the induction of the ferromagnetic-metallic state in the Ni-substituted and Cr-substituted samples are suggested to be due

to the induction of double-exchange interaction involving Ni^{2+}–O–Mn^{4+} and Mn^{3+}–O–Cr^{3+}, respectively. The variation in magnetic properties between the Ni-substituted and Cr-substituted samples is suggested to be due to the existence of different strengths of ferromagnetic interaction between Ni^{2+}–O–Mn^{4+} and Mn^{3+}–O–Cr^{3+}. In addition, the deviation of the temperature dependence of the inverse magnetic susceptibility curves from the Curie-Weiss law suggests the existence of Griffith's phase-like behaviour for both substitution samples. The Ni-substituted sample induced a greater GP effect than the Cr-substituted sample due to the larger difference of T_C and T_G value (T_C-T_G).

Keywords: Manganese Perovskites; Charge Ordered; Monovalent-Doped; Magnetic Ion; Griffith Phase

INTRODUCTION

Extensive research has been conducted on hole-doped perovskite ABO_3-type manganites with a general formula of $R_{1-x}A_xMnO_3$ (where R represents rare earth elements and A represents alkali or alkaline elements) due to their remarkable properties such as colossal magnetoresistance (CMR), ferromagnetic–paramagnetic (FM–PM) transition, and metal–insulator (MI) transition [1-5]. These properties are the result of the double-exchange (DE) interaction, where eg electrons are simultaneously transferred from Mn^{3+} ($t_{2g}^{3}\ e_g^{1}$) on O *p*-orbitals and from O *p*-orbitals to the empty eg orbital of Mn^{4+}($t_{2g}^{3}\ e_g^{0}$), favoring the ferromagnetic-metallic (FMM) state [5-6]. Conversely, the Jahn-Teller (JT) interaction related to Mn^{3+} ions promote paramagnetic insulating (PMI) behavior [6]. Understanding the physical behavior of doped manganites requires considering several other crucial factors such as phase separation (PS) [7-8], superexchange (SE) interaction [9], Griffith phase (GP) [10-12], and charge ordering (CO) [8-10]. Among these factors, CO has gained significant attention owing to its insulating and antiferromagnetic (AFM) behavior [12-14]. The CO state is observed in manganites doped with monovalent alkaline ions at a doping level of x = 0.25, such as in $Pr_{0.75}Na_{0.25}MnO_3$ (PNMO) [15-17]. The Coulomb interaction between Mn ions and the JT effect of Mn^{3+} ions lead to an alternately ordered arrangement of Mn^{3+} and Mn^{4+} ions in a 1:1 ratio at lattice sites, resulting in the localization of charge carriers and restricting

their mobility from hopping between lattice sites, which gives rise to an insulating behavior of the compound.

Several studies have shown that substituting elements at the Mn-site has a greater impact on the properties of manganites than substitution at the A-site, as Mn ions play a crucial role in their behavior [18-20]. Various factors, such as ionic configuration, spin states, and ionic radius of the substituting elements, can affect Mn-site substitution, resulting in different effects [21-24]. Substituting Mn with Cr^{3+} in $Pr_{0.5}Ca_{0.5}Mn_{1-x}Cr_xO_3$ [25] and $La_{0.5}Ca_{0.5}Mn_{1-x}Cr_xO_3$ [26] manganites effectively suppresses the CO state and replaces it with a FMM state. This is possible because Cr^{3+} ($t_{2g}^{3}\, e_g^{0}$) is involved in the DE interaction, having an ionic configuration similar to Mn^{4+} [25-26]. Substituting Ni^{2+} ($t_{2g}^{6}\, e_g^{2}$), which also has a pair of eg electrons, induces an MI transition. This is because of the SE FM interactions between Ni^{2+} and Mn^{4+} ions, which facilitates the DE interaction between Mn^{3+} and Mn^{4+} ions. Some studies suggest the presence of a DE-like interaction between Ni^{2+} and Mn^{4+} ions [27]. The effects of both magnetic ions, Ni and Cr substitution, especially in CO monovalent-doped manganites, have not been thoroughly investigated, and only a limited number of reports are available. Therefore, it is essential to study the effects of Ni and Cr substitution and its relationship with the induced FMM, particularly in monovalent-doped manganites.

The presence of the GP affects the behavior of manganites, causing an uneven distribution of ferromagnetic (FM) clusters in the paramagnetic (PM) region above TC [11, 28]. This phenomenon has been observed in several manganites, and can be identified by a deviation from Curie-Weiss behavior in the inverse of magnetic susceptibility versus temperature curve. GP behavior has been observed in $Pr_{0.5}Sr_{0.5}Mn_{1-y}Ga_yO_3$, suggesting the presence of FM clusters in the PM region. The exact nature of the GP phase is unclear, but it has been suggested that A-site disorder may contribute to different GP features. The effect of A-site substitution has been reported in manganites such as $Pr_{1-x}MnO_3$ [10] and $Pr_{0.7-y}Ho_ySr_{0.3}MnO_3$ [11]. However, there are no reports on the formation of GP in CO monovalent-doped Pr-based manganites. This study aims to investigate the effect of Ni^{2+} and Cr^{3+} substitution at the Mn-site on the structural and magnetic properties of CO d $Pr_{0.75}Na_{0.25}Mn_{1-x}A_xO_3$ (x = 0 and 0.03; A= Ni and Cr) manganite, and shed light on the mechanism of CO state suppression and FMM phase revival. The concentration of x = 0.03 was chosen based on the previous report [20,

27], which indicated that at x = 0.02, both substitutions of magnetic ions at the Mn-site were able to induce the CO state in the compound. In addition, the role of GP in these phenomena will also be discussed.

EXPERIMENTAL DETAILS

Polycrystalline samples of $Pr_{0.75}Na_{0.25}MnO_3$, $Pr_{0.75}Na_{0.25}Mn_{0.97}Ni_{0.03}O_3$ and $Pr_{0.75}Na_{0.25}Mn_{0.97}Cr_{0.03}O_3$ were prepared using the conventional solid-state synthesis method. In this project, high-purity (>99.99%) powders of Pr_6O_{11}, Na_2CO_3, Cr_2O_3, NiO and MnO_2 powders were weighed in a stoichiometric ratio using an electronic balance. These powders were mixed together and ground for 2 hours before calcined in air at 950 °C for 24 hours. Next, the powder was pressed into pellets (diameter: 13 mm; thickness: around 3 mm) under a pressure of around 5 tonnes and sintered in air at 1100 °C for 36 hours, with slow cooling at a rate of 1 °C/min to obtain the desired oxygen stoichiometry. The phase of the samples was characterized using an X-ray diffractometer (PANalytical model Xpert PRO MPD) with Cu-Kα (λ = 0.154 nm) radiation at room temperature. Data were collected in the 2θ range of 20 °–90 °. The magnetic transition temperatures (T_C) were obtained by measuring the AC susceptibility (χ') in the temperature range of 30 K to 300 K using a Stanford Research model SR-7265 lock-in amplifier.

RESULTS AND DISCUSSION

Figure 1 shows the XRD patterns and refinement for $Pr_{0.75}Na_{0.25}MnO_3$, $Pr_{0.75}Na_{0.25}Mn_{0.97}Ni_{0.03}O_3$ and $Pr_{0.75}Na_{0.25}Mn_{0.97}Cr_{0.03}O_3$ samples, including the Bragg reflection positions, and the measured and calculated intensities of the corresponding peaks at room temperature. The patterns reveal that all sample peaks appear at comparable angles and positions to those reported earlier for the parent compound of $Pr_{0.75}Na_{0.25}MnO_3$ manganite [15-16]. The Rietveld method was employed to refine the XRD data of the samples using the General Structure Analysis System (GSAS) program [29], the EXPGUI package, and VESTA [30]. The peaks were modelled using a pseudo-Voigt function, and the cell parameter and background function were also considered. The X-ray diffraction patterns of the samples (Figure 1) were subjected to final refinement at room temperature, revealing that all

the synthesized samples were single-phased and exhibited orthorhombic symmetry with Pnma space group (No. 62). The orthorhombic structure obtained in this study is consistent with prior findings on $Pr_{0.75}Na_{0.25}MnO_3$ manganites using the same refinement technique [15-16].

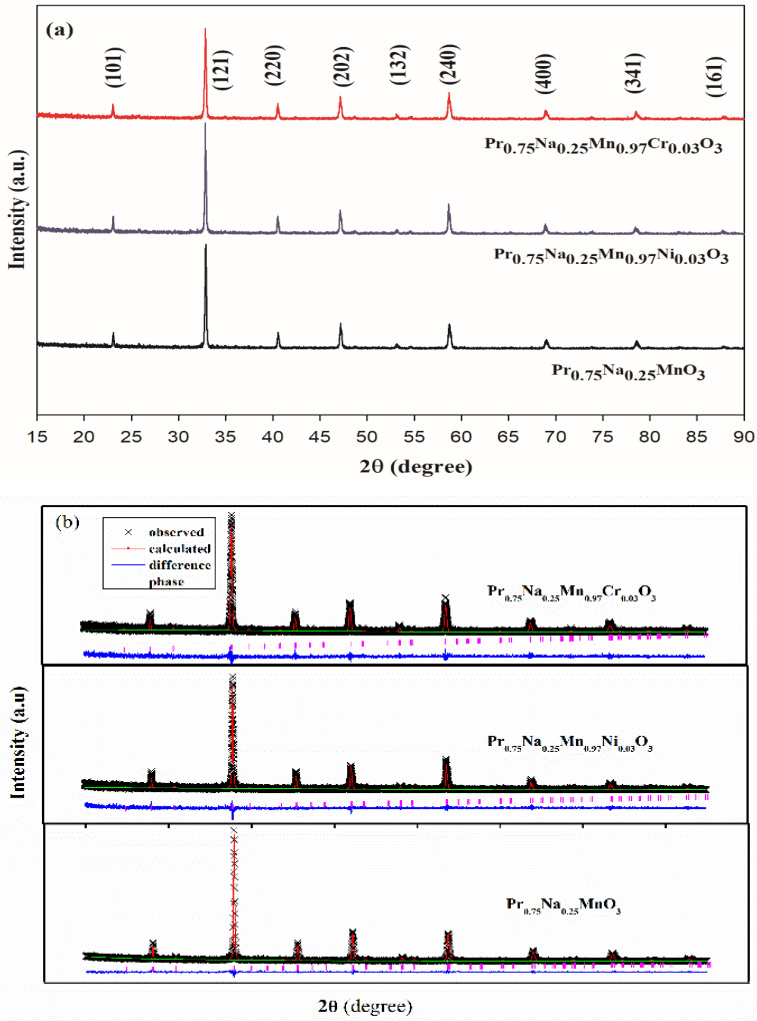

Figure 1: (a) X-ray Diffraction Pattern and (b) Final Refinement at room temperature for $Pr_{0.75}Na_{0.25}MnO_3$, $Pr_{0.75}Na_{0.25}Mn_{0.97}Ni_{0.03}O_3$ and $Pr_{0.75}Na_{0.25}Mn_{0.97}Cr_{0.03}O_3$ samples. Observed (cross black), calculated (continuous red line), difference between the observed and calculated data (blue line) and Bragg peak positions (vertical pink tick marks).

Table 1 provides a list of lattice parameters, calculated unit cell volume (V) and chi-squared (χ^2) values obtained from the final refinement of $Pr_{0.75}Na_{0.25}MnO_3$, $Pr_{0.75}Na_{0.25}Mn_{0.97}Ni_{0.03}O_3$ and $Pr_{0.75}Na_{0.25}Mn_{0.97}Cr_{0.03}O_3$ samples. The obtained structural parameter values for un-substituted sample, $Pr_{0.75}Na_{0.25}MnO_3$ are in agreement with those in previously reported on $Pr_{0.75}Na_{0.25}Mn_{1-x}Fe_xO_3$ [31] compound. The goodness of fit (GOF) indicator χ^2 suggests that there is a strong correspondence between the observed and calculated profiles, as demonstrated by the quality of refinement (as seen in Figure 1). The structural parameter values and calculated unit cell volume obtained for the un-substituted sample, $Pr_{0.75}Na_{0.25}MnO_3$ are consistent with those previously reported for $Pr_{0.75}Na_{0.25}MnO_3$ [31] compound. The calculated unit cell volume for samples with Ni substitution, $Pr_{0.75}N_{a0.25}Mn_{0.97}Ni_{0.03}O_3$ shows a slight increase to 228.54 Å^3. The small increase in unit cell volume suggests that Ni^{2+} may be replacing Mn3+ rather than Mn^{4+} in the crystal structure. This is likely due to the similar ionic radii of Ni^{2+} (0.69 Å) [32] and Mn^{3+} (0.65 Å) [32], both of which are relatively close compared to that of Mn^{4+} (0.56 Å). Similar observations have been reported in previous studies, such as in $Sm_{0.55}Sr_{0.45}Mn_{1-x}Ni_xO_3$ [32]. Meanwhile, it was found that the calculated unit cell volume for the Cr^{3+} substitution in $Pr_{0.75}Na_{0.25}Mn_{0.97}Cr_{0.03}O_3$, slightly decreased to V = 227.66 Å^3. This can be attributed to the smaller ionic radius (0.615 Å) of the Cr^{3+} ion continuously replacing the Mn^{3+} ion, which has a higher ionic radius (0.65 Å). Previous studies, such as $Sm_{0.55}Sr_{0.45}Mn_{1-x}Cr_xO_3$ [34], have reported similar observations.

The magnitude of MnO_6 octahedral distortion was determined by calculating the variance in JT denoted by σ^2_{JT}. This was achieved using the following Equation (1) [33]:

$$\sigma_{JT}^2 = \frac{1}{6}\left[\frac{d_{(Mn-O)i} - d_{<Mn-O>}}{d_{<Mn-O>}}\right]^2 \quad (1)$$

Here, d(Mn-O) represents the individual M-O bond distance, and d<Mn-O> represents the average Mn-O bond distance which obtained from Rietveld refinement. The calculated values of σ^2_{JT} decreased in both substituted samples, as shown in Table 1. The lower σ^2_{JT} value observed for the Ni-substituted sample, compared to the Cr-substituted sample could be attributed to the difference in their ionic radii.

Table 1: Structure parameters, unit cell volume, Goodness of Fit (GOF) value for refinement and JT Variance of $Pr_{0.75}Na_{0.25}MnO_3$, $Pr_{0.75}Na_{0.25}Mn_{0.97}Ni_{0.03}O_3$ and $Pr_{0.75}Na_{0.25}Mn_{0.97}Cr_{0.03}O_3$ samples. The number in the brackets represents uncertainty of the last digit.

Sample	$Pr_{0.75}Na_{0.25}MnO_3$	$Pr_{0.75}N_{a0.25}Mn_{0.97}Ni_{0.03}O_3$	$Pr_{0.75}Na_{0.25}Mn_{0.97}Cr_{0.03}O_3$
a (Å)	5.4378(5)	5.4469(5)	5.4367(5)
b (Å)	7.6867(7)	7.6969(6)	7.6831(7)
c (Å)	5.4488(6)	5.4511(6)	5.4409(5)
Volume, V ($Å^3$)	227.75(3)	228.54(2)	227.66(3)
GOF, χ^2	1.0510	1.7300	1.6110
Jahn-Teller Variance, σ_{JT}^2 (x 10^{-5} $Å^2$)	0.8150	0.4011	0.4331

Figure 2 displays the real part of the AC susceptibility plotted against temperature ($\chi'(T)$) for (a) $Pr_{0.75}Na_{0.25}MnO_3$ (b) $Pr_{0.75}Na_{0.25}Mn_{0.97}Ni_{0.03}O_3$ and (c) $Pr_{0.75}Na_{0.25}Mn_{0.97}Cr_{0.03}O_3$ samples in the temperature range of 30 K to 300 K. The inset is plot of $d\chi'/dT$ against T curve of each sample. The unsubstituted sample, $Pr_{0.75}Na_{0.25}MnO_3$, shows a weak ferromagnetic phase at low temperature. The wide peak observed at 210 K–240 K in the $\chi'(T)$ curve of the un-substituted sample (Figure 2(a)) is in agreement with previous studies that reported similar findings, pointing towards the existence of a CO transition in the $Pr_{0.75}Na_{0.25}MnO_3$ sample [17]. Additionally, a CO transition can be inferred from the observation of a broad peak at T_{CO}~212 K (see inset (a) in Figure 2)). The discovery aligns with Jirák *et al.,* [15] findings, where they also noted a wide peak at approximately 220 K for the $Pr_{0.75}Na_{0.25}MnO_3$ sample.

The presence observed at 212 K may be ascribed to the AFM phase, which could have resulted from the SE interaction between Mn ions, such as the interactions between the Mn^{3+}–O–Mn^{3+} and Mn^{4+}–O–Mn^{4+}. This suggestion is similar to previous findings for other CO manganites [28]. On the other hand, the substituted samples, $Pr_{0.75}Na_{0.25}MnO_3$, $Pr_{0.75}Na_{0.25}Mn_{0.97}Ni_{0.03}O_3$ and $Pr_{0.75}Na_{0.25}Mn_{0.97}Cr_{0.03}O_3$ exhibit a transition from ferromagnetic (FM) to paramagnetic (PM) behavior at low temperatures and display increased values of χ'. The transition temperature,

TC is indicated by the minimum peak in the dχ'/dT vs. T plot (see inset (b) and (c) in Figure 2). Table 1 shows that the observed transition temperature, as indicated by the minimum peak in the dχ'/dT vs. T plot, is 132 K for the Ni-substituted sample, $Pr_{0.75}Na_{0.25}Mn_{0.97}Ni_{0.03}O_3$ and at 147 K for the Cr-substituted sample, $Pr_{0.75}Na_{0.25}Mn_{0.97}Cr_{0.03}O_3$. The enhanced susceptibility and induced FM–PM transition for both substituted samples (Figure 2(b) and 2(c)) suggest that Ni^{2+} and Cr^{3+} effectively participate in strong FM interactions, which contribute to the enlargement of the FM phase at T_C below 132 K (Figure 2(b)) and below 147 K ((Figure 2(c)).

The absence of a similar broad peak in the χ'(T) curve (Figure 2(a)) indicates that the CO state is suppressed by the low concentration. The replacement of Ni^{2+} at the Mn^{3+} site could introduce additional exchange interactions involving Ni with Mn^{3+}–O–Ni^{2+}, Ni^{2+}–O–Mn^{4+} and N^{2+}–O–Ni^{2+} interactions. The presence of a FM phase implies that substituting Ni^{2+} at the Mn^{3+} site may disrupt the ordering of Mn^{3+} and Mn^{4+} ions, leading to a decrease in the local antiferromagnetic (AFM) phase related to CO. The FM super exchange (SE) interaction between Ni^{2+}–O–Mn^{4+} may also contribute to the development of the FM phase and enhance it. This interaction may reason for the higher T_C of the sample which Ni promotes a strong FM interaction. The introduction of Cr^{3+} ions has resulted in the suppression of the CO state and the formation of a ferromagnetic metallic (FMM) state. This is due to the involvement of Cr^{3+} ions in the double-exchange interaction, which is responsible for the formation of the FMM state. The replacement of Cr^{3+} at the Mn^{4+} site could introduce additional exchange interaction, Mn^{3+}–O–Cr^{3+}. The electronic configuration of Cr^{3+} ions is identical to that of Mn^{4+} ions, with both having a (t_{2g}^{3} e_g^{0}), configuration. This similarity allows Cr^{3+} ions to engage in the DE interaction, which is essential in facilitating the interaction between Mn^{3+} and Mn^{4+} ions. Earlier research has also proposed that Cr^{3+} plays a part in prompting the FMM phase in CO manganite [21-22].

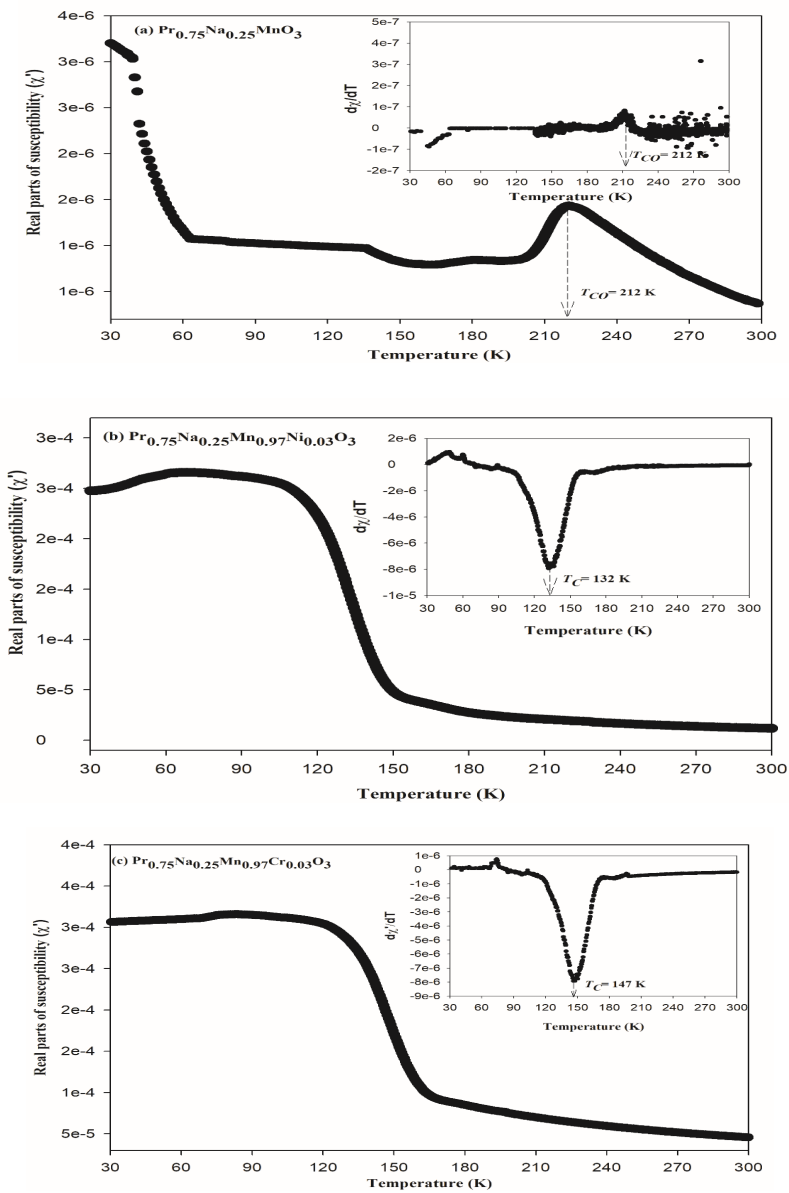

Figure 2: Real parts of AC susceptibility, χ' against temperature curves for (a) $Pr_{0.75}Na_{0.25}MnO_3$ (b) $Pr_{0.75}Na_{0.25}Mn_{0.97}Ni_{0.03}O_3$ and (c) $Pr_{0.75}Na_{0.25}Mn_{0.97}Cr_{0.03}O_3$ samples. Inset: Plot of dχ'/dT against T curve of each samples

Table 2: Curie Temperature (T_C), Charge Ordered Temperature (T_{CO}) and Griffiths Phase Temperature (T_G) of $Pr_{0.75}Na_{0.25}MnO_3$, $Pr_{0.75}Na_{0.25}Mn_{0.97}Ni_{0.03}O_3$ and $Pr_{0.75}Na_{0.25}Mn_{0.97}Cr_{0.03}O_3$samples.

Temperature (K)	$Pr_{0.75}Na_{0.25}MnO_3$	$Pr_{0.75}N_{a0.25}Mn_{0.97}Ni_{0.03}O_3$	$Pr_{0.75}Na_{0.25}Mn_{0.97}Cr_{0.03}O_3$
T_{CO}	218	-	-
T_C	-	132	147
T_G	-	148	160
T_G-T_C (difference)		16	13

For further investigation of magnetic properties of the samples, the temperature-dependent behavior of the inverse susceptibility, $1/\chi'(T)$ have been plotted. Figures 3(a)-3(c) display the temperature-dependent behavior of the inverse susceptibility, $1/\chi'(T)$, for $Pr_{0.75}Na_{0.25}MnO_3$, $Pr_{0.75}Na_{0.25}Mn_{0.97}Ni_{0.03}O_3$ and $Pr_{0.75}Na_{0.25}Mn_{0.97}Cr_{0.03}O_3$samples. The Curie-Weiss (CW) law characterizes the magnetic susceptibility of a ferromagnetic material in the paramagnetic (PM) region above the Curie point. In order to analyse the data, we fitted the experimental results of all samples to the Curie-Weiss law, which describes the temperature dependence of the magnetic susceptibility of a paramagnetic material in the absence of an external magnetic field [10-11]. The Curie-Weiss law is expressed as in Equation (2):

$$\chi' (M/H) = C/(T- \Theta) \quad (2)$$

where χ', Θ, and C represent the magnetic susceptibility, Curie-Weiss temperature, and Curie constant, respectively. Our analysis revealed that the Griffiths phase is characterized by a deviation from the Curie-Weiss behavior in the inverse magnetic susceptibility versus temperature curve.

The $1/\chi'(T)$ curve for un-substituted sample above 212 K (Figure 3(a)) followed the Curie-Weiss law behavior and the curve deviated from the linear behavior with decreasing temperature. Temperature dependence inverse magnetic susceptibility ($1/\chi'(T)$) curve for un-substituted sample follows the Curie-Weiss law behavior above 212 K, and the curve deviates above the linear line with decreasing temperature, hence indicating the existence of AFM phase. The AFM onset indicates the onset of CO at T_{CO} as CO state is an

AFM. Similar magnetic behavior has been reported in CO compounds [20, 31]. Figures 3(b) and 3(c) show the curves $1/\chi'(T)$ for substituted samples of $Pr_{0.75}Na_{0.25}Mn_{0.97}Ni_{0.03}O_3$(Figure 3(b)) and $Pr_{0.75}Na_{0.25}Mn_{0.97}Cr_{0.03}O_3$ (Figure 3(c)) samples. The curves slightly deviated from the Curie-Weiss law behavior above TC with a deviation temperature (TG). The TG value is 148 K for the Ni-substituted sample, $Pr_{0.75}Na_{0.25}Mn_{0.97}Ni_{0.03}O_3$ and at 160 K for the Cr-substituted sample, $Pr_{0.75}Na_{0.25}Mn_{0.97}Cr_{0.03}O_3$ (Table 2). The results of the observation imply that the substitution has the effect of suppressing the CO state while promoting the formation of ferromagnetic clusters which are regions of the material where the magnetic moments are aligned in the same direction [10]. These clusters appear to dominate in the substituted samples, indicating their importance in the compound's behavior. As a consequence, it is suggested that the formation of ferromagnetic clusters in the GP could potentially facilitate the occurrence of an FMM transition in the substituted samples. A typical feature of GP behavior, as reported in various manganites, is the observed deviation. However, in the case of $Pr_{0.75}Na_{0.25}Mn_{0.97}Ni_{0.03}O_3$, the $1/\chi'(T)$ curve exhibited a greater deviation between T_G and T_C (T_G - T_C) than $Pr_{0.75}Na_{0.25}Mn_{0.97}Cr_{0.03}O_3$, as presented in Table 2. This suggests that the sample contains a higher concentration of FM clusters.

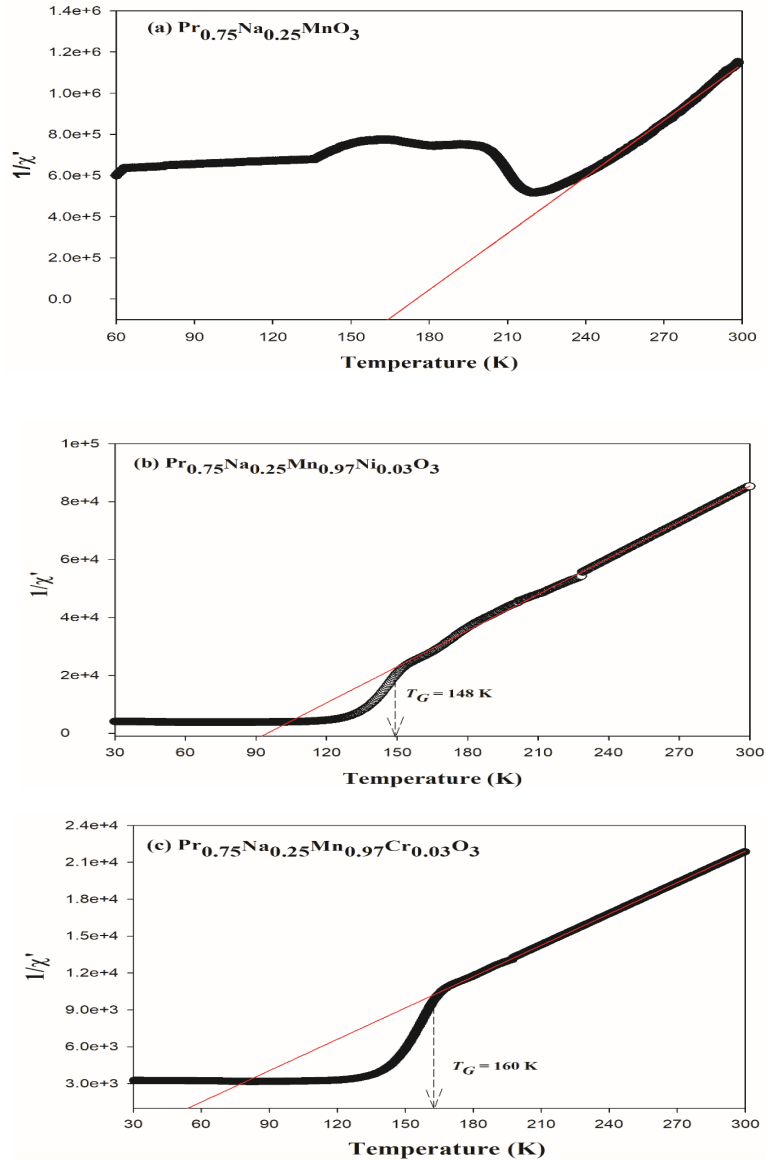

Figure 3: The Inverse of Magnetic Susceptibility versus Temperature, χ-1(T) Curve for (a) $Pr_{0.75}Na_{0.25}MnO_3$, (b) $Pr_{0.75}Na_{0.25}Mn_{0.97}Ni_{0.03}O_3$ and (c) $Pr_{0.75}Na_{0.25}Mn_{0.97}Cr_{0.03}O_3$ Samples. The Solid Red Lines are the Fitted Curve According to Curie-Weiss Law

CONCLUSION

In conclusion, the effects of Ni and Cr substitution at Mn-site on the structural and magnetic properties of CO $Pr_{0.75}Na_{0.25}Mn_{1-x}A_xO_3$ (x = 0 and 0.03; A= Ni and Cr) samples were studied to elucidate the influence of magnetic ions on the suppression of CO state and inducement of FMM phase. The findings showed that introducing a small amount of Ni and Cr (x = 0.03) significantly suppresses the CO state and induces FMM transition, indicating that both Ni^{2+} and Cr^{3+} can successfully induce DE interaction and FM phase. The replacement of Ni^{2+} at Mn^{3+} ion sites disturbed the local order of Mn ions, leading to a reduction in Coulomb interaction and JT distortion. This substitution also played a role in the FM SE interaction of Ni_{2+}–O–Mn^{4+}, facilitating the DE mechanism. On the other hand, due to the involvement of Cr^{3+} in the DE interaction, which has which has a similar ionic configuration to that of Mn^{4+}, Cr^{3+} also induced the FMM phase. Furthermore, the $1/\chi'(T)$ results revealed the formation of FM clusters in the PM region for both substituted samples. The recovery of the FMM state may have been facilitated by the GP behavior. The Ni-substituted sample induced a greater GP effect than the Cr-substituted sample due to the large difference in T_C and T_G value.

ACKNOWLEDGEMENTS

This work was supported by the Malaysian Ministry of Higher Education (MOHE) and Institute of Research Management and Innovation (IRMI), Universiti Teknologi MARA for providing fellowships and facilities to carry out the measurements [Ref: 600-RMC/GPM LPHD 5/3 (070/2021)].

REFERENCES

[1] L.P. Gor'kov & V.Z. Kresin, 2004. Mixed-valence manganites: Fundamentals and main properties. *Physics Reports*, 400(3), 149-208 .

[2] H. Wang, H. Zhang, K. Su, S. Huang, W. Tan, & D. Huo, 2020. Structure, charge ordering, and magnetic properties of perovskite $Sm_{0.5}Ca_{0.5}MnO_3$ manganite. *Journal of Materials Science: Materials in Electronics,* 31(17), 14421–14425 .

[3] C. Joël, B. Jean Francois & L. Ulrike, 2005. Development of new materials for spintronics. *Comptes Rendus Physique,* 6 (9), 977-996 .

[4] A. J. Millis, P. B. Littlewood & B. I. Shraiman, 1955. Double exchange alone does not explain the resistivity of $La_{1-x}Sr_xMnO_3$. *Physical Review Letters,* 74, 5144-5147 .

[5] J. M. D. Coey & M. Viret, 1999. Mixed-valence manganites, *Advances in Physics*, 48 (2), 167-293 .

[6] S. Herbert, A. Maignan, C. Martin & B. Raveau, 2001. Important role of impurity eg levels on the ground state of Mn-site doped manganites. *Solid State Communications*, 121, 229-234 .

[7] E. Dagotto, T. Hotta & A. Moreo, 2001. Colossal magnetoresistance materials; The key role of phase separation. *Physics Reports*, 344(1-3), 1-153 .

[8] B. Raveau, M. Herviu, A. Maignan & C. Martin, 2001. The route to CMR manganites: What about charge ordering and phase separation?. *Journal of Materials Chemistry,* 11, 29-36 .

[9] C. Zener, 1951. Interaction between the d-Shells in the transition metals. II Ferromagnetic compounds of manganese with perovskite structure. *Journal of Physical Review*, 82, 403-405 .

[10] A. N. Ulyanov, A. V. Sidorov, A. V. Vasiliev, N. E. Pismenova & E. A. Goodilin, 2017. Electron structure, Raman “vacancy” modes and Griffiths-like phase of self-doped Pr1-xMnO3+δ manganites. *Journal of Alloys and Compounds,* 722, 77-82 .

[11] N. Rama, M. Opel, V. Sankaranarayanan, R. Gross, S. B. Ogale, T. Venkatesan & R. Ramachandra, 2005. A-site dependent percolative thermopower and Griffiths phase in $Pr_{0.7-x}Ho_xSr0_{.3}MnO_3$ (x = 0.0, 0.04, 0.08 and 0.1). *Journal of Applied Physics*, 97, 13-1–13-3 .

[12] H. Yoshizawa, Y. Tomioka & Y. Tokura, 2003. Novel stripe-type charge ordering in the metallic A-type antiferromagnet $Pr_{0.5}Sr_{0.5}MnO_3$. *Physica*

B, 329 (18), 679–680 .

[13] Y. Tomioka, T. Okuda, Y. Okimoto, A. Asamitsu, H. Kuwahara & Y. Tokura, 2001. Charge/orbital ordering in perovskite manganites. *Journals of Alloys and Compounds*. 326 (1-2), 27-35 .

[14] L. Yu, C. Qian & Q. Dawei, 2013. Effects of Al doping upon ac susceptibility of $Pr_{0.5}Ca_{0.5}MnO_3$. *Ceramics International,* 39(2), 1345-1350 .

[15] X. H. Zhang, 2005. Magnetic properties and charge ordering in $Pr_{0.75}Na_{0.25}MnO_3$ manganite. *Journal of Solid State Communications*, 135(6), 356-360 .

[16] Z. Jir'ak Z, J. Hejtm'anek, K. Knizek, E. Pollert, M. Dlouha, S. Vratislav, R. Kuzel & M. Hervieu, 2005. Structure and magnetism in the $Pr_{1-x}Na_xMnO_3$ perovskites ($0 \leq x \leq 0.2$). *Journals of Magnetism and Magnetic Materials*, 250, 275-287.

[17] Y. Wang H. Zhang, H. Wang, D. Yang, S. Huang, K. Su, W. Tan & D. Huo, 2021. Charge ordering and magnetic properties of $La_xSm_{0.5-x}Ca_{0.5}MnO_3$ manganite. *The Journal of Materials Science: Materials in Electronics,* 32(14), 18721–18727 .

[18] L. Yi, K. Hui & Z. Changfei, 2007. Coexistence of charge ordering and ferromagnetism in $Nd_{0.5}Ca_{0.5}Mn_{1-x}Co_xO_3$ ($x \leq 0.1$). J*ournals of Alloys and Compounds*, 439 (1-2), 33-36 .

[19] X. Zhang & Z. Li, 2011. Influence of Cr-doping on the magnetic and electrical transport properties of $Nd_{0.75}Na_{0.25}MnO_3$. *Journal of Rare Earths*, 29(3), 230-234 .

[20] R. Rozilah, N. Ibrahim & A.K. Yahya, 2019. Inducement of ferromagnetic–metallic phase and magnetoresistance behavior in charged ordered monovalent-doped $Pr_{0.75}Na_{0.25}MnO_3$ manganite by Ni substitution. *Solid State Sciences,* 87, 64-80 .

[21] A. Martinelli, M. Ferretti, C. Castellano, M.R. Cimberle & C. Ritter, 2008. Crystal and magnetic structure of Cr- and Ni-substituted ($La_{0.50}Ca_{0.50}$)MnO_3. *Journal of Physics: Condensed Matter,* 20 (14), 145210 (10pp).

[22] A. Ammar, S. Zouari & A. Cheikhrouhou, 2013. Structural and magnetic properties of chromium doped manganites. *Journal of Alloys and Compounds*, 354(1), 85-90 .

[23] I. Dhiman, A. Das, A. K. Nigam & U. Gasser, 2011 Influence of B-site disorder in $La_{0.5}Ca_{0.5}Mn_{1-x}B_xO_3$ (B = Fe, Ru, Al and Ga) manganites. *Journal of Physics: Condensed Matter,* 23, 246006 .

[24] S. Shamsuddin, Abdel-Baset M.A. Ibrahim & A. K. Yahya, 2013. Effects of Cr substitution and oxygen reduction on elastic anomaly and ultrasonic velocity in charge-ordered $Nd_{0.5}Ca_{0.5}Mn_{1-x}Cr_xO_3$. *Ceramics International*, 39, S185–S188 .

[25] L. Pi, S. H´ebert, C. Yaicle, C. Martin, A. Maignan & B. Raveau, 2003. The $Pr_{0.5}Ca_{0.5}Mn_{1-x}Cr_xO_3$ series ($0 \leq x \leq 0.5$): evidence of steps in the magnetic and transport properties for a narrow composition range. *Journal of Physics: Condensed Matter,* 13515(17), 2701–2709 .

[26] O. Toulemonde, F. Studera, A. Barnabe, A. Maignan, C. Martin & B. Raveau, 1998(2014). Charge states of transition metal in Cr, Co and Ni doped $Ln_{0.5}Ca_{0.5}MnO_3$ CMR manganites. T*he European Physical Journal B,* 4(2), 159-167 .

[27] M. Arifin, N. Ibrahim, Z. Mohamed, A. K. Yahya, Nawazish A. Khan & M. Nasir Khan, 2018. Revival of Metal-Insulator and Ferromagnetic-Paramagnetic Transitions by Ni Substitution at Mn Site in Charge-Ordered Monovalent Doped $Nd_{0.75}Na_{0.25}MnO_3$ manganites. *Journal of Superconductivity and Novel Magnetism,* 31(1), 2851-2868.

[28] R. Rozilah, N. Ibrahim, Z. Mohamed, A. K. Yahya, Nawazish A. Khan & M. Nasir Khan, 2017. Inducement of ferromagnetic-metallic phase in intermediate-doped charge-ordered $Pr_{0.75}Na_{0.25}MnO_3$ manganite by K^+ substitution. *Physica B: Condensed Matter*, 521, 281–294 .

[29] B. H. Toby, 2001. EXPGUI, a graphical user interface for GSAS. *Journal of Applied Crystallography,* 34, 210-213

[30] K. Momma & F. Izumi, 2008. VESTA: A three-dimensional visualization system for electronic and structural analysis. J*ournal of Applied Crystallography*, 1441(3), 653-658 .

[31] E. Elyana, Z. Mohamed , S.A. Kamil, S.N. Supardan , S. K. Chen & A. K. Yahya, 2018. Revival of ferromagnetic behavior in charge-ordered $Pr_{0.75}Na_{0.25}MnO_3$ manganite by ruthenium doping at Mn site and its MR effect. J*ournal of Solid State Chemistry,* 258, 191–200 .

[32] R. D. Shannon, 1976. Revised effective ionic radii and systematic studies of interatomic distances in Halides and Chaleogenides. *Acta Crystallographica,* 32, 751-767 .

[33] R. R. Zhang, G. L. Kuang, X. Luo & Y. P. Sun, 2009. Structural, magnetic and electrical transport properties of V doped $Bi_{0.3}Ca_{0.7}MnO_{3.}$ *Journals of Alloys and Compounds,* 484(1-2), 36–39 .

[34] M. M. Abdelhadi & K. A. Ziq, 2011. Effect of Nickel Doping on the Magnetotransport Properties of $Sm_{0.55}Sr_{0.45}MnO_3$ Manganites, *Journal of Superconductivity and Novel Magnetism*, 24, 319–323 .